BIOCHEMISTRY
including biophysical chemistry & molecular biology

Article

pubs.acs.org/biochemistry

DNA-*N*-Glycosylases Process Novel *O*-Glycosidic Sites in DNA

Suzanne J. Admiraal and Patrick J. O'Brien*

Department of Biological Chemistry, University of Michigan Medical School, Ann Arbor, Michigan 48109-0600, United States

Supporting Information

ABSTRACT: After the hydrolysis of the *N*-glycosyl bond between a damaged base and C1′ of a deoxyribosyl moiety of DNA, human alkyladenine DNA glycosylase (AAG) and *Escherichia coli* 3-methyladenine DNA glycosylase II (AlkA) bind tightly to their abasic DNA products, potentially protecting these reactive species. Here we show that both AAG and AlkA catalyze reactions between bound abasic DNA and small, primary alcohols to form novel DNA-*O*-glycosides. The synthesis reactions are reversible, as the DNA-*O*-glycosides are converted back into abasic DNA upon being incubated with AAG or AlkA in the absence of alcohol. AAG and AlkA are therefore able to hydrolyze *O*-glycosidic bonds in addition to *N*-glycosyl bonds. The newly discovered DNA-*O*-glycosidase activities of both enzymes compare favorably with their known DNA-*N*-glycosylase activities: AAG removes both methanol and 1,N^6-ethenoadenine (εA) from DNA with single-turnover rate constants that are 2.9×10^5-fold greater than the corresponding uncatalyzed rates, whereas the rate enhancement of 3.7×10^7 for removal of methanol from DNA by AlkA is 300-fold greater than its rate enhancement for removal of εA from DNA. Although the biological significance of the DNA-*O*-glycosidase reactions is not known, the evolution of new DNA repair pathways may be aided by enzymes that practice catalytic promiscuity, such as these two unrelated DNA glycosylases.

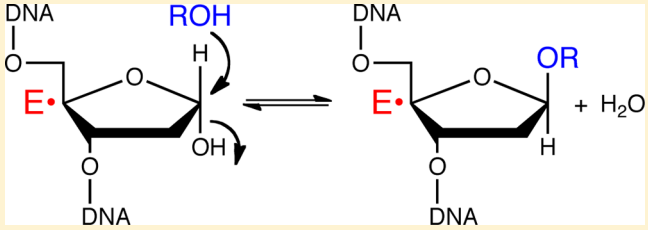

An abasic site is formed within DNA when the *N*-glycosyl bond between a nucleobase and deoxyribose is hydrolyzed. This scission is promoted when the *N*-glycosyl bond is destabilized by nearby chemical modifications, such as alkylation of the nucleobase by alkylating agents.[1] Abasic sites are formed enzymatically by DNA glycosylases that remove specific damaged bases, and subsequent enzymes of the base excision repair (BER) pathway ultimately restore the original DNA sequence by replacing the deoxyribosyl phosphate moiety with the nucleotide that is complementary to the unpaired opposing nucleotide. Unrepaired abasic lesions can interfere with DNA replication, transcription, and topoisomerase activity, resulting in mutagenesis or toxicity.[2] The abasic site can also access an unstable open-chain aldehyde form that readily cross-links with amines or undergoes β-elimination accompanied by DNA strand breakage.[3−5]

Many DNA glycosylases, including AAG and AlkA, bind tightly to their abasic DNA products.[6−12] Such tight binding has been proposed to shield this reactive DNA intermediate from side reactions until it is further processed by downstream enzymes of the BER pathway.[2] We explored the effect of binding to AAG and AlkA on the reactivity of abasic DNA by exposing glycosylase−abasic DNA complexes to small alcohols. Remarkably, both DNA glycosylases catalyzed the formation of alcohol−DNA adducts. The adducts contain an *O*-glycosidic linkage between a hydroxyl group of the alcohol and C1′ of the deoxyribose, based on their resistance to alkaline hydrolysis. These results reveal that the reactive environments of their active sites provide AAG and AlkA with the capacity for *O*-glycosidic bond synthesis and highlight the susceptibility of abasic DNA to damage, even when it is glycosylase-bound.

The DNA-*O*-glycosides synthesized by AAG and AlkA were tested as substrates for breakdown by AAG and AlkA. Alcohols were efficiently excised from the DNA-*O*-glycosides by both enzymes, extending the known substrate range of DNA glycosylases to include sites of DNA damage with alcohol substitutions at C1′ of deoxyribose.

EXPERIMENTAL PROCEDURES

Chemicals. Glycerol, ethanol, methanol, 2-propanol, 1-propanol, ethylene glycol, 1,2-propanediol, 1,3-propanediol, and 1,N^6-ethenoadenine (εA) were from Sigma-Aldrich.

Purification of Recombinant Proteins. Wild-type and E125Q mutant forms of truncated human AAG lacking the first 79 amino acids were expressed in *Escherichia coli* and purified as previously described.[13] Full-length *E. coli* AlkA was produced as a C-terminal six-His-tagged protein from a modified pET24 vector that encoded a TEV cleavage site. D238N AlkA was generated by site-directed mutagenesis. Both wild-type and D238N mutant AlkA proteins were purified with NTA-Ni^{2+}; the tags were removed with TEV protease, and the proteins were further purified using source S cation exchange. Peak fractions were dialyzed into storage buffer containing 50 mM NaHEPES (pH 7.5), 100 mM NaCl, 0.1 mM EDTA, and 1 mM DTT and stored at −80 °C.

Received: February 19, 2013
Revised: May 10, 2013
Published: May 20, 2013

Preparation of Oligonucleotides. The 25mer duplex ab-DNA substrate was prepared by combining equal concentrations of 5′-(FAM)-CGATAGCATCCTabCCTTCTCTCC-AT-3′, an oligonucleotide with a centrally located abasic site (ab) and a 5′-fluorescein (FAM) label, and its complement, 5′-ATGGAGAGAAGGTAGGATGCTATCG-3′. The unlabeled oligonucleotide was synthesized by IDT and the labeled oligonucleotide by the Keck Center at Yale University (New Haven, CT). Standard protecting groups were used in both syntheses, and deprotection was conducted according to the manufacturer's recommendations (Glen Research), with one exception. The lesion-containing oligonucleotide was initially supplied with an *O*-*tert*-butyldimethylsilyl (*O*-TBDMS) protecting group on C1′ of its central deoxyribosyl group. Both oligonucleotides were desalted using Sephadex G-25 and purified using denaturing polyacrylamide gel electrophoresis as previously described.[14] The *O*-TBDMS protecting group was subsequently removed in an 80% acetic acid/20% water mixture; after neutralization, the deprotected oligonucleotide was desalted using Sephadex G-25. Denaturing polyacrylamide gel electrophoresis of the deprotected oligonucleotide that had been subjected to alkaline hydrolysis at 70 °C showed that ∼98% of the 25mer was cleaved into 12mer, consistent with deprotection of the central deoxyribosyl group to an abasic site. The concentrations of the oligonucleotide containing an abasic site and its complement were determined from their absorbances at 260 nm using calculated extinction coefficients prior to annealing. Preliminary experiments with ab-DNA prepared conventionally, via treatment of a uracil-containing oligonucleotide with uracil DNA glycosylase,[15] gave the same results as those performed with the ab-DNA described above. The authentic 25mer duplex εdA-DNA was prepared as previously described.[15]

Preparation and Isolation of Alcohol−DNA Adducts for the Study of Their Breakdown by AlkA and AAG. Preparative reaction mixtures contained 50 mM NaMES (pH 6.5), 100 mM NaCl, 0.1 mg/mL BSA, 1 mM EDTA, 1 mM TCEP, 2.5 M alcohol, 0.5 μM ab-DNA, and 2 μM AlkA or AAG in volumes of 100 μL. Reaction mixtures for preparing the propanol−DNA adduct contained 1 M propanol, because higher concentrations of propanol inactivated both AlkA and AAG. Control reactions without alcohol were performed and the mixtures processed alongside reaction mixtures that contained alcohol. Reaction mixtures were incubated at 37 °C for 4 h (AlkA reactions) or 20−48 h (AAG reactions). DNA was isolated from the remaining reaction components by phenol/chloroform extraction followed by gel filtration on MicroSpin G-25 columns (GE Healthcare). The alcohol−DNA adducts are also stable to standard ethanol precipitation conditions and can be isolated using this method.[16] Because the alcohol reactions proceeded to concentration-dependent end points rather than to completion, each final preparation consisted of 5−20% alcohol−DNA adduct and 80−95% unreacted ab-DNA.

Synthesis of *N*-Glycosyl and *O*-Glycosidic Linkages within DNA by AAG (for Figure 1). Reaction mixtures containing 50 mM NaMES (pH 6.5), 100 mM NaCl, 0.1 mg/mL BSA, 1 mM EDTA, 1 mM TCEP, 2 μM AAG, and 0.5 μM ab-DNA were supplemented with 5 mM εA, 2.5 M glycerol, or no additive and incubated at 37 °C for 20 h. A control reaction mixture containing 2.5 M glycerol and all other reaction components except AAG was also used. Reactions were quenched with sodium hydroxide to give a final concentration of 0.2 M. The quenched samples were heated at 70 °C for 10 min to quantitatively cleave abasic sites and subsequently mixed with an equal volume of formamide/EDTA loading buffer. All samples were loaded and separated on a 20% (w/v) polyacrylamide sequencing gel containing 6.6 M urea. The gel was scanned using a Typhoon Trio imager (GE Healthcare), and emission was measured with a 520BP40 filter following excitation of the fluorescein label at 488 nm.

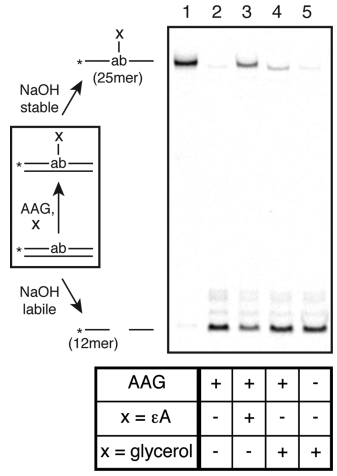

Figure 1. AAG synthesizes *N*-glycosyl and *O*-glycosidic linkages within DNA. The image shows a fluorescence scan of samples that were subjected to alkaline hydrolysis prior to separation on a 20% denaturing polyacrylamide gel. The original reaction mixtures were incubated at 37 °C for 20 h and contained 50 mM NaMES (pH 6.5), 100 mM NaCl, 0.1 mg/mL BSA, 1 mM EDTA, 1 mM TCEP, and 0.5 μM ab-DNA; the presence or absence of 2 μM AAG, 5 mM εA, and 2.5 M glycerol in the original reaction mixtures is indicated in the chart for samples in lanes 2−5. Lane 1 contained an authentic sample of the εdA-DNA 25mer, which is slightly less mobile than the glycerol−DNA 25mer (lane 4) under these conditions. In the scheme, ab represents the abasic site, x is εA or glycerol, and the asterisk denotes the location of the 5′-fluorescein label. The fraction of εdA-DNA in lane 3 is 0.40, and the fraction of glycerol−DNA adduct in lane 4 is 0.08.

Single-Turnover Alcohol−DNA Adduct Synthesis and Breakdown Assays for AAG and AlkA. Reactions were conducted at 37 °C in 50 mM NaMES (pH 6.5), 100 mM NaCl, 0.1 mg/mL BSA, 1 mM EDTA, and 1 mM TCEP. Typical reaction mixtures contained 10−100 nM DNA (ab-DNA or an alcohol−DNA adduct), 0.2−1 μM enzyme (AAG or AlkA), and 0−2.5 M alcohol; the observed rate constants did not change when the enzyme concentration was increased, confirming that single-turnover kinetics were monitored under these conditions. Reactions were initiated by adding a small volume of enzyme to the remaining reaction components in a final volume of 20−40 μL. Aliquots were withdrawn at various times and their reactions quenched with sodium hydroxide to give a final concentration of 0.2 M. The quenched samples were heated at 70 °C for 10 min to quantitatively cleave abasic sites. Samples were mixed with an equal volume of formamide/EDTA loading buffer and run on 15% (w/v) polyacrylamide sequencing gels containing 6.6 M urea. Gels were scanned using a Typhoon Trio imager (GE Healthcare), and emission was measured with a 520BP40 filter following excitation of the fluorescein label at 488 nm. Fluorescence intensities of gel bands were quantified using ImageQuant TL (GE Healthcare) and corrected for the amount of background signal. The data were converted to fraction alcohol−DNA adduct [fraction

dx.doi.org/10.1021/bi400218j | *Biochemistry* 2013, 52, 4066−4074

alcohol−DNA adduct = [alcohol−DNA adduct]/([alcohol−DNA adduct] + [ab-DNA])] and then fit by a single exponential. For reactions of E·ab-DNA and alcohol, the single exponential included a zero point of 0.02, to reflect the amount of nonhydrolyzable DNA in reaction mixtures without alcohol, and an end point term: fraction alcohol−DNA adduct = end point$[1 - \exp(-k_{obs}t)]$ + 0.02, where k_{obs} is the observed rate constant and t is time. For E·alcohol−DNA reactions, the single exponential included a term representing the initial fraction of alcohol−DNA adduct in each preparation and an end point term, to reflect the amount of nonhydrolyzable DNA: fraction alcohol−DNA adduct = (fraction alcohol−DNA adduct)$_{init}[\exp(-k_{obs}t)]$ + end point, where k_{obs} is the observed rate constant and t is time. In all cases, the nonlinear least-squares fit was good ($R > 0.98$).

RESULTS

Glycosylase-Catalyzed Reactions of Abasic DNA with Alcohols. In previous work, we showed that AAG catalyzes formation of an *N*-glycosyl linkage between εA and DNA containing an abasic site.[15] The 25mer ab-DNA undergoes β,δ-elimination at its abasic position and is converted to a 12mer upon being subjected to alkaline hydrolysis, whereas DNA that has covalently incorporated εA (εdA-DNA) remains stable (Figure 1, lanes 1−3). By analogy, we reasoned that it may be possible to identify novel substrates for AAG by incubating it with ab-DNA and small molecules that are not known to be excised from DNA by AAG; the accumulation of DNA adducts that are stable to alkaline hydrolysis would provide evidence of AAG-dependent covalent incorporation of such molecules into DNA at C1′ of the base-free deoxyribosyl moiety. When AAG was incubated with ab-DNA in the presence of glycerol, a base-stable adduct was observed (Figure 1, lane 4). The adduct did not form when AAG was omitted from the reaction mixture (Figure 1, lane 5), and the amount of adduct that formed increased as the concentration of glycerol in the synthesis reaction mixture was increased (Figure S1 of the Supporting Information).

The simplest model for formation of the glycerol−DNA species is one in which glycerol can occupy the nucleobase binding pocket of AAG when ab-DNA is bound in the active site. Although the anomeric form of ab-DNA that binds to AAG is unknown, it is widely assumed that the *N*-glycosylase activity of AAG entails direct displacement of a damaged base by water to initially form the α-anomer. Nucleophilic attack by glycerol on the α-anomer of ab-DNA would result in a β-anomeric cyclic acetal, which contains an *O*-glycosidic linkage between C1′ of the deoxyribosyl moiety and a hydroxyl group of glycerol (Figure 2). The stability of the glycerol−DNA adduct to alkaline hydrolysis (Figure 1, lane 4) is consistent with this chemical linkage, because model conjugates of ADP-ribose containing a similar acetal linkage between C1′ of the ribosyl moiety and hydroxyl groups of small alcohols are known to be base-stable.[17,18] The attacking hydroxyl group is likely to be one of the two equivalent primary hydroxyl groups of glycerol, because 1-propanol but not 2-propanol reacts like glycerol (see below). To the best of our knowledge, the conversion of ab-DNA and glycerol to RO−DNA by AAG represents the first example of *O*-glycosidic bond synthesis by a DNA-*N*-glycosylase. The AAG-catalyzed reaction shown in Figure 2 is reminiscent of the *N*-glycosyl bond synthesis reaction that AAG catalyzes between ab-DNA and the nucleobase εA to form εdA-DNA.[15]

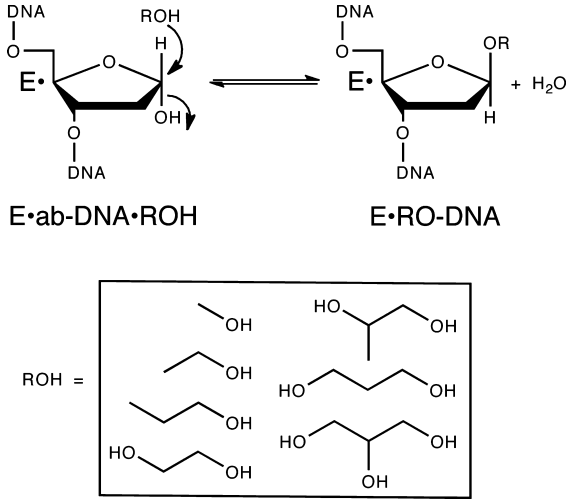

Figure 2. Model for the reversible reaction of E·ab-DNA with an alcohol molecule (ROH) under single-turnover conditions, where all of the DNA present is bound to E and E represents AAG or AlkA. Alcohols that have been shown to react in this study are boxed.

To explore the generality of *O*-glycosidic bond synthesis by DNA-*N*-glycosylases, we surveyed the effects of various alcohols in reactions of AAG or the structurally unrelated AlkA. Both glycosylases formed DNA adducts between ab-DNA and methanol, ethanol, 1-propanol, ethylene glycol, 1,2-propanediol, 1,3-propanediol, or glycerol (alcohol structures shown in Figure 2). The DNA adduct made in reaction mixtures containing methanol, the smallest alcohol, could be resolved from the DNA adduct made in reaction mixtures containing glycerol, the largest alcohol, by denaturing polyacrylamide gel electrophoresis, directly demonstrating that AAG and AlkA can incorporate different alcohols into abasic DNA (Figure S2 of the Supporting Information). The amount of alcohol−DNA adduct increased with time for each combination of enzyme and alcohol, as shown for the AlkA-catalyzed reaction between glycerol and ab-DNA in Figure 3A. Neither enzyme formed a DNA adduct between ab-DNA and the secondary alcohol 2-propanol, even though its size and intrinsic reactivity are comparable to those of other alcohols, suggesting that the flexibility of primary alcohols is an important factor for the synthesis reactions.

The AlkA-catalyzed syntheses were significantly faster and resulted in higher product yields than the AAG-catalyzed syntheses, so the dependence of each AlkA reaction on alcohol concentration was investigated. As shown for the glycerol reaction in Figure 3B and for the other alcohols in Figure S3 of the Supporting Information, reactions of AlkA·ab-DNA and alcohols proceeded to higher end points as the concentration of alcohol increased. These end points appear to represent internal equilibria[19] between the AlkA-bound ab-DNA (AlkA·ab-DNA) and the AlkA-bound alcohol−DNA adduct (AlkA·alcohol−DNA), because addition of more AlkA after the apparent internal equilibrium is established has no effect on the amount of alcohol−DNA adduct present (Figure S4 of the Supporting Information), whereas dilution of alcohol decreases the amount of alcohol−DNA adduct present (Figure S5 of the Supporting Information).

The ratios of alcohol−DNA adduct to ab-DNA at the end points of reactions of AlkA·ab-DNA and alcohols are plotted as a function of the alcohol to water ratios in Figure 3C, where the

dx.doi.org/10.1021/bi400218j | *Biochemistry* 2013, 52, 4066−4074

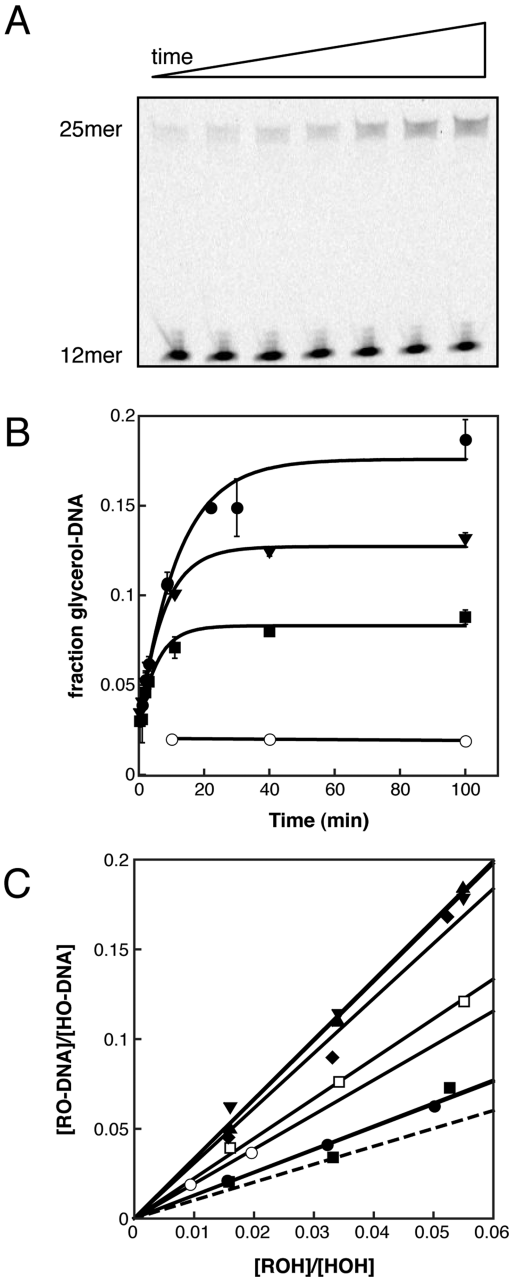

Figure 3. Synthesis of the alcohol−DNA adduct by AlkA. (A) The amount of glycerol−DNA 25mer increases with time in a representative reaction mixture that contained 1 μM AlkA, 100 nM ab-DNA, and 2.5 M glycerol. The reaction was performed at 37 °C in 50 mM NaMES (pH 6.5), 100 mM NaCl, 0.1 mg/mL BSA, 1 mM EDTA, and 1 mM TCEP, and reactions were quenched and mixtures subjected to alkaline hydrolysis prior to separation on a 15% denaturing polyacrylamide gel. The fraction of glycerol−DNA adduct at each time point was determined, and these data are included with data from duplicate 2.5 M glycerol reactions in panel B (●). (B) The amount of glycerol−DNA adduct at the reaction end point increases as the concentration of glycerol increases in reaction mixtures containing 1 μM AlkA, 100 nM ab-DNA, and 0.8 (■), 1.7 (▼), or 2.5 M glycerol (●). A no enzyme control reaction mixture containing 100 nM ab-DNA and 2.5 M glycerol (○) is also shown. All reaction mixtures were incubated at 37 °C and contained 50 mM NaMES (pH 6.5), 100 mM NaCl, 0.1 mg/mL BSA, 1 mM EDTA, and 1 mM TCEP. Exponential fits to the data are shown, but we have not interpreted rate constants for the synthesis reactions because of the presumed solvent effects at high glycerol concentrations (see the legend of Figure S3 of the Supporting Information). (C) The ratio of alcohol−DNA adduct (RO−DNA) to ab-DNA (HO−DNA) at the end point of reactions of AlkA·ab-DNA and alcohol increases linearly as a function of the ratio of alcohol (ROH) to water (HOH) present. Concentrations of methanol (●), ethanol (■), propanol (○), 1,2-propanediol (□), ethylene glycol (◆), 1,3-propanediol (▲), or glycerol (▼) ranged from 0.5 to 2.5 M in the various reaction mixtures (panel B and Figure S3 of the Supporting Information). The water concentration does not remain constant when the alcohol concentration is varied over this wide range, so the ratio of alcohol concentration to water concentration ([ROH]/[HOH]) is plotted on the *x*-axis rather than simply alcohol concentration. The identity reaction of water is shown as a dashed line with a slope of 1.

identity reaction of water is shown as a dashed line with a slope of 1. Saturation of the alcohol reactions with respect to the end point is not observed, suggesting that AlkA lacks well-defined binding sites for the alcohols and preventing the values for K_{int}, the internal equilibrium constants, from being obtained. Therefore, the maximal ratio of alcohol−DNA adduct to ab-DNA shown in Figure 3C for each alcohol is a lower limit for the value of K_{int} for reaction of that alcohol. Interestingly, there is an apparent clustering of the slopes for the end point concentration dependencies that correlates with the structures of the alcohols. Slopes close to the identity slope of 1 are observed for methanol and ethanol, which are small, monohydroxylic alcohols with pK_a values similar to the pK_a of water. The propanol and 1,2-propanediol reactions result in a slope near 2, suggesting that these slightly larger molecules may be more favorably positioned for reaction with ab-DNA than are the small nucleophiles. The even steeper slopes of ∼3 for the reactions of ethylene glycol, 1,3-propanediol, and glycerol may reflect both a size advantage and a statistical advantage arising from their equivalent primary hydroxyl groups.

Alcohol−DNA Adducts Are Substrates for AAG and AlkA. The alcohol−DNA adducts synthesized by AlkA and AAG are novel DNA-*O*-glycosides, and their reactions are expected to be reversible. Therefore, they were tested as substrates for these DNA-*N*-glycosylases. The complete set of seven alcohol−DNA adducts was synthesized preparatively in reaction mixtures containing AlkA, ab-DNA, and alcohols. AlkA and the alcohols were subsequently removed from the preparations by phenol/chloroform extraction and gel filtration, respectively. The glycerol−DNA adduct was also prepared using AAG, to address the question of whether the adducts made by AlkA and AAG are identical.

The amount of alcohol−DNA adduct decreased with time for each combination of wild-type AAG and alcohol−DNA adduct, as shown for a representative reaction of the glycerol−DNA adduct (Figure 4A, left). However, no conversion of glycerol−DNA adduct into ab-DNA by the active site mutant E125Q AAG, which lacks the general base that is required for the *N*-glycosylase reaction,[13,20,21] could be detected under the same conditions (Figure 4A, right). This result confirms that wild-type AAG, not a contaminating enzyme, is responsible for the DNA-*O*-glycosidase activity, because E125Q AAG prepared and tested in the same way has no activity. The representative reactions of the glycerol−DNA adduct were quantified, and the resulting data points were combined with data from equivalent reactions in Figure 4B. The kinetics of glycerol−DNA adduct breakdown are monophasic, suggesting that the adduct is a single species, and wild-type AAG converts it into ab-DNA with

dx.doi.org/10.1021/bi400218j | *Biochemistry* 2013, 52, 4066−4074

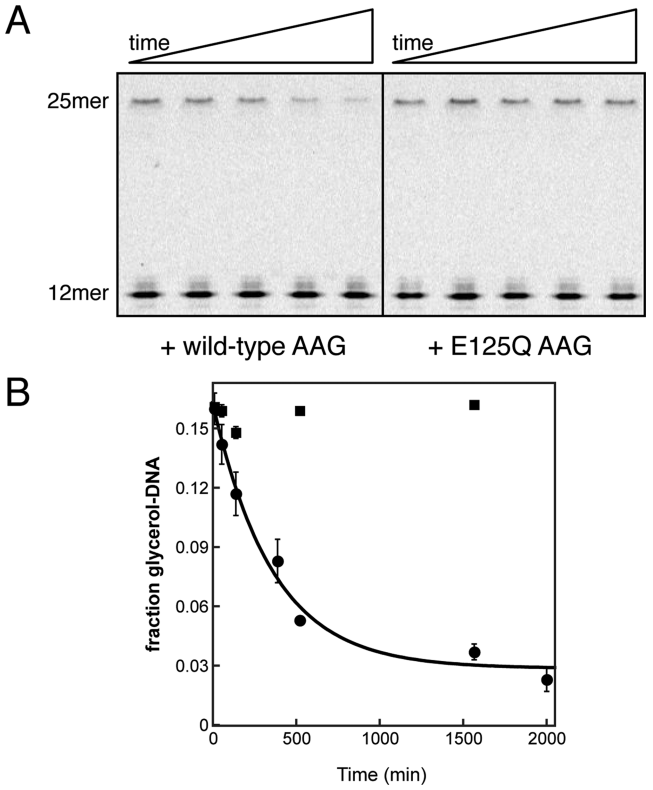

Figure 4. Glycerol−DNA adduct is a substrate for wild-type AAG. (A) The amount of glycerol−DNA 25mer decreased with time in a representative reaction mixture that contained 250 nM wild-type AAG and a 50 nM glycerol−DNA adduct preparation (from AlkA synthesis, 16% glycerol−DNA adduct and 84% ab-DNA) but stayed constant in an analogous reaction mixture that contained 250 nM E125Q AAG. Reactions were quenched and mixtures subjected to alkaline hydrolysis prior to separation on a 15% denaturing polyacrylamide gel. The fraction of glycerol−DNA adduct at each time point was determined, and these data are included with data from equivalent reactions in panel B. (B) The amount of the glycerol−DNA adduct decreases with a single-turnover rate constant of 0.0029 min^{-1} in the presence of wild-type AAG (●), but no breakdown of the glycerol−DNA adduct was detected in analogous reaction mixtures containing E125Q AAG (■). Reactions were performed at 37 °C in 50 mM NaMES (pH 6.5), 100 mM NaCl, 0.1 mg/mL BSA, 1 mM EDTA, and 1 mM TCEP.

a rate constant of 0.0029 min^{-1}. The presence of multiple species that react with identical rate constants is unlikely but cannot be ruled out. Analogous results were obtained for the other alcohol−DNA adducts (Figure S6 of the Supporting Information), and the single-turnover rate constants for their breakdown by AAG are summarized in Table 1.

Like AAG, wild-type AlkA excises alcohols from the glycerol−DNA adduct (Figure 5) and the other alcohol−DNA adducts (Figure S6 of the Supporting Information). The active site mutant D238N AlkA, which lacks the general base that is important for the *N*-glycosylase reaction,[22,23] has little or no activity (Figure 5A, right), indicating that the observed DNA-*O*-glycosidase activity belongs to wild-type AlkA, not to a contaminant. The kinetics of alcohol−DNA adduct breakdown by AlkA are monophasic (Figure 5B and Figure S6 of the Supporting Information), as observed for AAG (see above), providing additional evidence that each alcohol adduct consists of a single species. The presence of multiple species that react with identical rate constants is unlikely but cannot be ruled out. The single-turnover rate constants for the breakdown of

Table 1. Rate Constants for Hydrolysis of Alcohol−DNA Adducts by DNA Glycosylases

	k_{st} (min^{-1})[a]	
	AAG	AlkA
ethanol−DNA	0.0041	0.59
ethylene glycol−DNA	0.0027	0.31
glycerol−DNA	0.0029	0.21
methanol−DNA	0.0044	0.56
1,2-propanediol−DNA	0.0026	0.22
1,3-propanediol−DNA	0.012	0.39
propanol−DNA	0.0089	0.83

[a]Single-turnover rate constants for the release of alcohols opposite T in 25mer duplex DNA with a saturating enzyme level were measured at 37 °C in NaMES (pH 6.5). Measurements are the average of at least two independent determinations, and the standard deviation is ≤25% of the value.

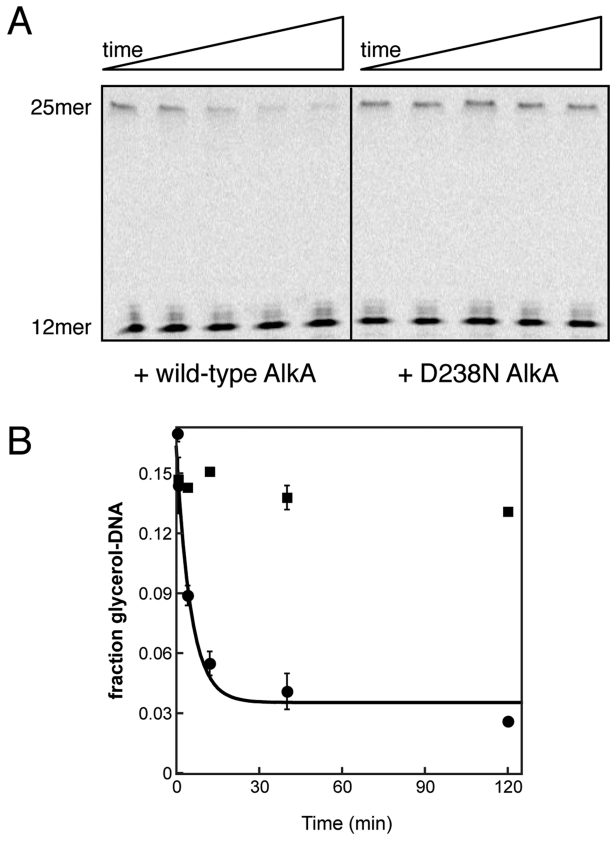

Figure 5. Glycerol−DNA adduct is a substrate for wild-type AlkA. (A) The amount of glycerol−DNA 25mer decreases with time in a representative reaction mixture that contained 250 nM wild-type AlkA and a 50 nM glycerol−DNA adduct preparation (from AlkA synthesis, 16% glycerol−DNA adduct and 84% ab-DNA), but the glycerol−DNA adduct is at least 100-fold less reactive in an analogous reaction mixture that contained 250 nM D238N AlkA. Reactions were quenched and mixtures subjected to alkaline hydrolysis prior to separation on a 15% denaturing polyacrylamide gel. The fraction of glycerol−DNA adduct at each time point was determined, and these data are included with data from equivalent reactions in panel B. (B) The amount of the glycerol−DNA adduct decreases with a single-turnover rate constant of 0.21 min^{-1} in the presence of wild-type AlkA (●), but little breakdown of the glycerol−DNA adduct was detected in analogous reaction mixtures containing D238N AlkA (■). Reactions were performed at 37 °C in 50 mM NaMES (pH 6.5), 100 mM NaCl, 0.1 mg/mL BSA, 1 mM EDTA, and 1 mM TCEP.

dx.doi.org/10.1021/bi400218j | *Biochemistry* 2013, 52, 4066−4074

alcohol−DNA substrates by AlkA range from 0.21 to 0.83 min^{-1} and are 30−150-fold larger than the corresponding rate constants for the AAG-catalyzed reactions (Table 1).

The glycerol−DNA adduct prepared using AlkA was the substrate for the reactions shown in Figures 4 and 5. For comparison, the glycerol−DNA adduct was also prepared using AAG. The breakdown of the glycerol−DNA adduct from the two independent preparations was investigated with both AAG (Figure 6A) and AlkA (Figure 6B). The reaction of each enzyme with either preparation is indistinguishable, after normalization to account for the different initial percentages of the glycerol−DNA adduct in the two preparations (Figure 6, insets). This is strong evidence that AlkA and AAG synthesize identical glycerol−DNA species.

DISCUSSION

Glycosylases Accelerate the Reaction of Abasic DNA with Alcohols. Our results reveal that binding to AAG or AlkA promotes the reaction of abasic DNA with alcohols to form DNA-*O*-glycosides. High concentrations of alcohols were used to facilitate detection of alcohol−DNA adducts using our gel-based assay, but analogous reactions to form and process related DNA-*O*-glycosides may be biologically relevant at much lower levels. Simple estimates indicate that formation of approximately one DNA-*O*-glycoside lesion per human cell per day is possible (see the Supporting Information). Although DNA-*O*-glycosides are predicted to be rare in human cells, it is important to note that use of even a single such site as a template during replication of the genome has the potential to introduce a harmful mutation. This is because DNA-*O*-glycosides are expected to be miscoding, as are fragmented nucleotides in DNA.[24−26]

The reactions that AAG and AlkA catalyze between alcohols and C1′ of the deoxyribosyl moiety of abasic DNA could yield DNA-*O*-glycosides that are *β*-anomeric cyclic acetals, *α*-anomeric cyclic acetals, or a combination of both configurations. However, both the synthesis and the breakdown reactions of the DNA-*O*-glycosides are monophasic, suggesting that only one of the two anomeric forms predominates. Attack of an alcohol at C1′ of bound *α*-anomeric abasic DNA from within the nucleobase binding pocket would produce a *β*-anomeric DNA-*O*-glycoside, as depicted in Figure 2, whereas attack of an alcohol at C1′ of bound *β*-anomeric abasic DNA would produce the *α*-anomeric alternative. We favor the former model, in which AAG and AlkA synthesize the *β*-anomeric DNA-*O*-glycosides, because the *O*-glycosidic bonds of the predominant species are readily hydrolyzed by AAG and AlkA, which are both known to hydrolyze the *N*-glycosyl bonds of damaged *β*-anomeric nucleotides, but not those of *α*-anomeric nucleotides.

The AAG- and AlkA-catalyzed reactions of small alcohols with abasic DNA could be detected and characterized in this study because of the stability of the cyclic acetal products. It is highly likely that the same reaction that occurs between alcohols and abasic DNA within the glycosylase active sites also occurs with water, whereby water reacts with *α*-anomeric abasic DNA to form *β*-anomeric abasic DNA. However, this water reaction has not been verified because the *α*- and *β*-anomeric cyclic hemiacetals are in equilibrium in solution (60:40 *α*:*β*),[27] where they interconvert via a reactive aldehyde form.[3]

Although ours is the first report of *O*-glycosidic bond synthesis by DNA-*N*-glycosylases and is notable because the products of these reactions are potentially mutagenic DNA adducts, similar enzymatic reactions between alcohols and small molecule substrates have previously been observed. Several enzymes that hydrolyze the *N*-glycosyl bond between a nitrogenous base and a simple ribosyl- or deoxyribosyl-containing moiety can incorporate methanol instead of water at C1 of the sugar-containing product.[28−37]

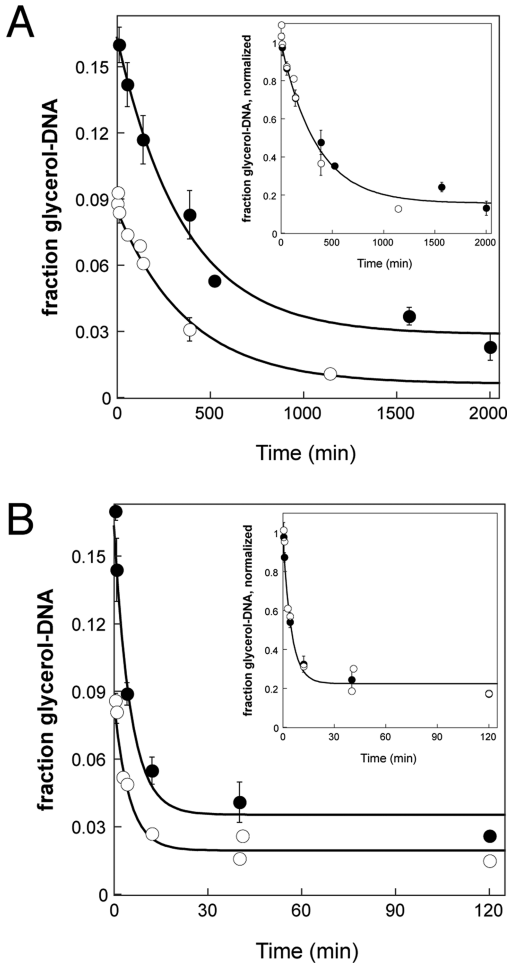

Figure 6. Glycerol−DNA adducts synthesized by AlkA or by AAG react identically. (A) Breakdown of glycerol−DNA adducts synthesized by AlkA (●) or AAG (○) by wild-type AAG. The two preparations have different initial percentages of the glycerol−DNA adduct, because each synthesis reaction proceeded to a concentration-dependent end point rather than to completion. To more easily compare glycerol−DNA adducts from the two preparations, the inset shows the same data after the fraction of glycerol−DNA adduct at each time point was normalized relative to the fraction of glycerol−DNA adduct present at time zero for that preparation (0.16 for the glycerol−DNA adduct synthesized by AlkA; 0.08 for the glycerol−DNA adduct synthesized by AAG). The time courses were indistinguishable after normalization, so data from both preparations were combined to calculate the rate constant of 0.0029 min^{-1} for conversion of the glycerol−DNA adduct to ab-DNA by AAG (Table 1). (B) Breakdown of glycerol−DNA adducts synthesized by AlkA (●) or AAG (○) by wild-type AlkA. The inset shows the normalized data, as described for panel A. The time courses were indistinguishable after normalization, so data from both preparations were combined to calculate the rate constant of 0.21 min^{-1} for conversion of the glycerol−DNA addduct to ab-DNA by AlkA (Table 1). Reactions were performed at 37 °C in 50 mM NaMES (pH 6.5), 100 mM NaCl, 0.1 mg/mL BSA, 1 mM EDTA, and 1 mM TCEP.

dx.doi.org/10.1021/bi400218j | *Biochemistry* 2013, 52, 4066−4074

Table 2. Rate Enhancement for the Release of Damaged Moieties from DNA by AlkA and AAG

	enzymatic		nonenzymatic	rate enhancement[a]	
molecule released	k_{st} (min^{-1}), AlkA	k_{st} (min^{-1}), AAG	k_{non} (min^{-1})	AlkA	AAG
methanol	5.6×10^{-1} [b]	4.4×10^{-3} [b]	1.5×10^{-8} [c]	3.7×10^{7}	2.9×10^{5}
εA	7.5×10^{-2} [d]	2.0×10^{-1} [e]	7.0×10^{-7} [e]	1.1×10^{5}	2.9×10^{5}

[a]Rate enhancement is defined as k_{st}/k_{non}. [b]For release of methanol opposite T in 25mer duplex DNA at 37 °C and pH 6.5 (from Table 1). [c]For release of methanol from 1-*O*-methyl-2-deoxy-D-ribose, extrapolated to 37 °C (from ref 41). [d]For release of εA opposite T in 25mer duplex DNA at 37 °C and pH 6.0 (from ref 23). [e]For release of εA opposite T in 25mer duplex DNA at 37 °C and pH 6.0 (from ref 42).

Practical Implications for DNA Repair Studies. The discovery that glycerol and other alcohols react with abasic DNA bound to AAG and AlkA has practical implications. AAG and AlkA are structurally unrelated, yet both enzymes catalyze the same reaction to form DNA-*O*-glycosides, so it seems likely that this reaction is also catalyzed by other DNA-*N*-glycosylases. Glycerol is frequently added to biochemical solutions to stabilize proteins, and glycerol or diols are often present at high concentrations during protein crystallography as precipitants or cryoprotectants. Indeed, several crystal structures of the DNA-*N*-glycosylase UDG show glycerol in the uracil binding site.[38−40] Small alcohols should be used cautiously in studies of the BER pathway, given their potential to react with abasic DNA and thus complicate the interpretation of experimental results. Alcohol−DNA adducts are likely to be overlooked in routine assays because of their similarities to normal oligonucleotides that contain nitrogenous bases. For example, they are stable to treatments that cause strand cleavage at abasic sites, as are normal oligonucleotides, and they comigrate with normal oligonucleotides on denaturing gels run under standard conditions.

Novel DNA-*O*-Glycoside Substrates for AlkA and AAG. Our results demonstrate that alcohols can be removed from DNA by DNA glycosylases AlkA and AAG. The rate enhancements for *O*-glycoside hydrolysis by AlkA and AAG can be estimated by comparing the enzyme-catalyzed rate constants for release of methanol from the methanol−DNA adduct to the nonenzymatic rate constant for release of methanol from the model substrate 1-*O*-methyl-2-deoxy-D-ribose (Table 2).[41] For AlkA, the rate enhancement of 3.7×10^7 is 300-fold greater than the rate enhancement for release of the damaged base εA from DNA. For AAG, the same rate enhancement of 2.9×10^5 is obtained for *O*-glycoside hydrolysis of the methanol−DNA adduct and for *N*-glycosyl hydrolysis of εdA-DNA. These robust rate enhancements for *O*-glycoside hydrolysis likely reflect the fact that both AAG and AlkA have binding pockets that allow them to excise damaged nucleobases of varying sizes.[23,42] Therefore, they are able to accommodate the replacement of nucleobase leaving groups with alcohol leaving groups.

The E125Q AAG and D238N AlkA active site mutants lack the carboxylate group that their wild-type counterparts use as general bases to activate a water nucleophile, so the abilities of these mutants to hydrolyze the *N*-glycosyl bonds of damaged nucleotides are substantially decreased.[13,20−23] As described above, little or no conversion of the glycerol−DNA adduct into ab-DNA by E125Q AAG (Figure 4) or D238N AlkA (Figure 5) could be detected under the same conditions in which the corresponding reactions catalyzed by the wild-type glycosylases had proceeded to completion. These results suggest that the same carboxylate side chains that activate water for AAG- and AlkA-catalyzed hydrolysis of *N*-glycosyl bonds also activate water for AAG- and AlkA-catalyzed hydrolysis of *O*-glycosidic bonds.

In addition to the hydrolysis of alcohol−DNA adducts by the monofunctional DNA glycosylases AAG and AlkA reported herein, slow cleavage of the β-anomer of a methanol−DNA adduct by the bifunctional pyrimidine dimer DNA glycosylase from T4 bacteriophage has been detected.[43] Although the biological significance of this class of DNA-*O*-glycoside substrates is unknown, their breakdown by three unrelated DNA glycosylases highlights the capacity to develop novel DNA repair mechanisms in response to a changing environment. Many other DNA repair enzymes also exhibit catalytic promiscuity, as would be expected if new enzymatic activities have been recruited for DNA repair throughout evolution.[44]

■ ASSOCIATED CONTENT

Supporting Information

Figures S1−S6 and a calculation for estimating the frequency of formation of DNA-*O*-glycosides in human cells, as described in the text. This material is available free of charge via the Internet at http://pubs.acs.org.

■ AUTHOR INFORMATION

Corresponding Author

*Department of Biological Chemistry, University of Michigan Medical School, 1150 W. Medical Center Dr., Ann Arbor, MI 48109-0600. E-mail: pjobrien@umich.edu. Telephone: (734) 647-5821. Fax: (734) 763-4581.

Funding

This work was supported in part by National Institutes of Health Grant RO1 CA122254 to P.J.O.

Notes

The authors declare no competing financial interest.

■ ACKNOWLEDGMENTS

We thank members of the O'Brien lab for helpful discussions and critical reading of the manuscript.

■ ABBREVIATIONS

AAG, human alkyladenine DNA glycosylase (also known as MPG, methylpurine DNA glycosylase); AlkA, 3-methyladenine DNA glycosylase II; εA, 1,N^6-ethenoadenine; BER, base excision repair; BSA, bovine serum albumin.

■ REFERENCES

(1) Loeb, L. A., and Preston, B. D. (1986) Mutagenesis by apurinic/apyrimidinic sites. *Annu. Rev. Genet. 20*, 201−230.

(2) Friedberg, E. C., Walker, G. C., Siede, W., Wood, R. D., Schultz, R. A., and Ellenberger, T. (2006) *DNA repair and mutagenesis*, ASM Press, Washington, DC.

(3) Lhomme, J., Constant, J. F., and Demeunynck, M. (1999) Abasic DNA structure, reactivity, and recognition. *Biopolymers 52*, 65−83.

(4) Dutta, S., Chowdhury, G., and Gates, K. S. (2007) Interstrand cross-links generated by abasic sites in duplex DNA. *J. Am. Chem. Soc. 129*, 1852−1853.
(5) Johnson, K. M., Price, N. E., Wang, J., Fekry, M. I., Dutta, S., Seiner, D. R., Wang, Y., and Gates, K. S. (2013) On the formation and properties of interstrand DNA-DNA cross-links forged by reaction of an abasic site with the opposing guanine residue of 5′-CAp sequences in duplex DNA. *J. Am. Chem. Soc. 135*, 1015−1025.
(6) Waters, T. R., and Swann, P. F. (1998) Kinetics of the action of thymine DNA glycosylase. *J. Biol. Chem. 273*, 20007−20014.
(7) Porello, S. L., Leyes, A. E., and David, S. S. (1998) Single-turnover and pre-steady-state kinetics of the reaction of the adenine glycosylase MutY with mismatch-containing DNA substrates. *Biochemistry 37*, 14756−14764.
(8) Petronzelli, F., Riccio, A., Markham, G. D., Seeholzer, S. H., Stoerker, J., Genuardi, M., Yeung, A. T., Matsumoto, Y., and Bellacosa, A. (2000) Biphasic kinetics of the human DNA repair protein MED1 (MBD4), a mismatch-specific DNA N-glycosylase. *J. Biol. Chem. 275*, 32422−32429.
(9) Abner, C. W., Lau, A. Y., Ellenberger, T., and Bloom, L. B. (2001) Base excision and DNA binding activities of human alkyladenine DNA glycosylase are sensitive to the base paired with a lesion. *J. Biol. Chem. 276*, 13379−13387.
(10) O'Neill, R. J., Vorob'eva, O. V., Shahbakhti, H., Zmuda, E., Bhagwat, A. S., and Baldwin, G. S. (2003) Mismatch uracil glycosylase from *Escherichia coli*: A general mismatch or a specific DNA glycosylase? *J. Biol. Chem. 278*, 20526−20532.
(11) Pettersen, H. S., Sundheim, O., Gilljam, K. M., Slupphaug, G., Krokan, H. E., and Kavli, B. (2007) Uracil-DNA glycosylases SMUG1 and UNG2 coordinate the initial steps of base excision repair by distinct mechanisms. *Nucleic Acids Res. 35*, 3879−3892.
(12) Zhao, B., and O'Brien, P. J. (2011) Kinetic mechanism for the excision of hypoxanthine by *Escherichia coli* AlkA and evidence for binding to DNA ends. *Biochemistry 50*, 4350−4359.
(13) O'Brien, P. J., and Ellenberger, T. (2003) Human alkyladenine DNA glycosylase uses acid-base catalysis for selective excision of damaged purines. *Biochemistry 42*, 12418−12429.
(14) Hedglin, M., and O'Brien, P. J. (2008) Human alkyladenine DNA glycosylase employs a processive search for DNA damage. *Biochemistry 47*, 11434−11445.
(15) Admiraal, S. J., and O'Brien, P. J. (2010) N-glycosyl bond formation catalyzed by human alkyladenine DNA glycosylase. *Biochemistry 49*, 9024−9026.
(16) Sambrook, J., Fritsch, E. F., and Maniatis, T. (1989) *Molecular Cloning: A Laboratory Manual*, 2nd ed., Cold Spring Harbor Laboratory Press, Plainview, NY.
(17) Cervantes-Laurean, D., Loflin, P. T., Minter, D. E., Jacobson, E. L., and Jacobson, M. K. (1995) Protein modification by ADP-ribose via acid-labile linkages. *J. Biol. Chem. 270*, 7929−7936.
(18) Cervantes-Laurean, D., Jacobson, E. L., and Jacobson, M. K. (1997) Preparation of low molecular weight model conjugates for ADP-ribose linkages to protein. *Methods Enzymol. 280*, 275−287.
(19) Fersht, A. (1999) *Structure and Mechanism in Protein Science*, W. H. Freeman and Co., New York.
(20) Lau, A. Y., Schärer, O. D., Samson, L., Verdine, G. L., and Ellenberger, T. (1998) Crystal structure of a human alkylbase-DNA repair enzyme complexed to DNA: Mechanisms for nucleotide flipping and base excision. *Cell 95*, 249−258.
(21) Lau, A. Y., Wyatt, M. D., Glassner, B. J., Samson, L. D., and Ellenberger, T. (2000) Molecular basis for discriminating between normal and damaged bases by the human alkyladenine glycosylase, AAG. *Proc. Natl. Acad. Sci. U.S.A. 97*, 13573−13578.
(22) Labahn, J., Scharer, O. D., Long, A., Ezaz-Nikpay, K., Verdine, G. L., and Ellenberger, T. E. (1996) Structural basis for the excision repair of alkylation-damaged DNA. *Cell 86*, 321−329.
(23) O'Brien, P. J., and Ellenberger, T. (2004) The *Escherichia coli* 3-methyladenine DNA glycosylase AlkA has a remarkably versatile active site. *J. Biol. Chem. 279*, 26876−26884.
(24) Evans, J., Maccabee, M., Hatahet, Z., Courcelle, J., Bockrath, R., Ide, H., and Wallace, S. (1993) Thymine ring saturation and fragmentation products: Lesion bypass, misinsertion and implications for mutagenesis. *Mutat. Res. 299*, 147−156.
(25) Maccabee, M., Evans, J. S., Glackin, M. P., Hatahet, Z., and Wallace, S. S. (1994) Pyrimidine ring fragmentation products. Effects of lesion structure and sequence context on mutagenesis. *J. Mol. Biol. 236*, 514−530.
(26) McNulty, J. M., Jerkovic, B., Bolton, P. H., and Basu, A. K. (1998) Replication inhibition and miscoding properties of DNA templates containing a site-specific cis-thymine glycol or urea residue. *Chem. Res. Toxicol. 11*, 666−673.
(27) Chen, J., Dupradeau, F. Y., Case, D. A., Turner, C. J., and Stubbe, J. (2008) DNA oligonucleotides with A, T, G or C opposite an abasic site: Structure and dynamics. *Nucleic Acids Res. 36*, 253−262.
(28) Pascal, M., and Schuber, F. (1976) The stereochemistry of calf spleen NAD-glycohydrolase-catalyzed NAD methanolysis. *FEBS Lett. 66*, 107−109.
(29) Oppenheimer, N. J. (1978) The stereospecificity of pig brain NAD-glycohydrolase-catalyzed methanolysis of NAD. *FEBS Lett. 94*, 368−370.
(30) Yost, D. A., and Anderson, B. M. (1983) Adenosine diphosphoribose transfer reactions catalyzed by *Bungarus fasciatus* venom NAD glycohydrolase. *J. Biol. Chem. 258*, 3075−3080.
(31) Tarnus, C., Muller, H. M., and Schuber, F. (1988) Chemical evidence in favor of a stabilized oxocarbonium-ion intermediate in the NAD^+ glycohydrolase-catalyzed reactions. *Bioorg. Chem. 16*, 38−51.
(32) Muller-Steffner, H. M., Augustin, A., and Schuber, F. (1996) Mechanism of cyclization of pyridine nucleotides by bovine spleen NAD^+ glycohydrolase. *J. Biol. Chem. 271*, 23967−23972.
(33) Zhang, B., Muller-Steffner, H., Schuber, F., and Potter, B. V. (2007) Nicotinamide 2-fluoroadenine dinucleotide unmasks the NAD^+ glycohydrolase activity of *Aplysia californica* adenosine 5′-diphosphate ribosyl cyclase. *Biochemistry 46*, 4100−4109.
(34) Kline, P. C., and Schramm, V. L. (1995) Pre-steady-state transition-state analysis of the hydrolytic reaction catalyzed by purine nucleoside phosphorylase. *Biochemistry 34*, 1153−1162.
(35) Berthelier, V., Tixier, J. M., Muller-Steffner, H., Schuber, F., and Deterre, P. (1998) Human CD38 is an authentic $NAD(P)^+$ glycohydrolase. *Biochem. J. 330* (Part 3), 1383−1390.
(36) Sauve, A. A., Munshi, C., Lee, H. C., and Schramm, V. L. (1998) The reaction mechanism for CD38. A single intermediate is responsible for cyclization, hydrolysis, and base-exchange chemistries. *Biochemistry 37*, 13239−13249.
(37) Doddapaneni, K., Zahurancik, W., Haushalter, A., Yuan, C., Jackman, J., and Wu, Z. (2011) RCL hydrolyzes 2′-deoxyribonucleoside 5′-monophosphate via formation of a reaction intermediate. *Biochemistry 50*, 4712−4719.
(38) Xiao, G., Tordova, M., Jagadeesh, J., Drohat, A. C., Stivers, J. T., and Gilliland, G. L. (1999) Crystal structure of *Escherichia coli* uracil DNA glycosylase and its complexes with uracil and glycerol: Structure and glycosylase mechanism revisited. *Proteins 35*, 13−24.
(39) Leiros, I., Moe, E., Lanes, O., Smalas, A. O., and Willassen, N. P. (2003) The structure of uracil-DNA glycosylase from Atlantic cod (*Gadus morhua*) reveals cold-adaptation features. *Acta Crystallogr. D59*, 1357−1365.
(40) Schormann, N., Grigorian, A., Samal, A., Krishnan, R., DeLucas, L., and Chattopadhyay, D. (2007) Crystal structure of vaccinia virus uracil-DNA glycosylase reveals dimeric assembly. *BMC Struct. Biol. 7*, 45.
(41) Wolfenden, R., Lu, X., and Young, G. (1998) Spontaneous hydrolysis of glycosides. *J. Am. Chem. Soc. 120*, 6814−6815.
(42) O'Brien, P. J., and Ellenberger, T. (2004) Dissecting the broad substrate specificity of human 3-methyladenine-DNA glycosylase. *J. Biol. Chem. 279*, 9750−9757.
(43) McCullough, A. K., Sanchez, A., Dodson, M. L., Marapaka, P., Taylor, J. S., and Lloyd, R. S. (2001) The reaction mechanism of DNA glycosylase/AP lyases at abasic sites. *Biochemistry 40*, 561−568.

(44) O'Brien, P. J. (2006) Catalytic promiscuity and the divergent evolution of DNA repair enzymes. *Chem. Rev. 106*, 720−752.